

ALICE ZDC and TCTTVB Tertiary Collimators - reminders

- Zero-degree calorimeters in the heavy-ion experiments (ALICE, CMS, ATLAS) are crucial for physics measurements
 - Measure energy carried away by non-interacting (spectator) beam nucleons
 - D1 separator magnet separates spectator protons and neutrons to two distinct calorimeters 92 m from IP
 - Neutron calorimeter also measures neutrons from electromagnetic dissociation (1 and 2 n)
- Physics measurements affected:
 - The energy mean value and resolution
 - centrality determination
 - The ϕ azimuthal angle distribution
 - measurement of the reaction plane in nuclear collisions and therefore measurement of the directed flow
- Angular spread of spectator neutrons from nuclear Fermi momentum

Transverse divergence of spectator neutrons

Nuclear radius: $R_A \approx (1.25 \text{ fermi})A^{1/3}$

Nucleon density: $n \approx \frac{A}{\frac{4}{3}\pi R_A^3}$

Fermi energy: $E_f = \frac{\hbar^2}{2m_n} \left(\frac{3\pi^2 n}{2} \right)^{2/3} \approx 30 \text{ MeV}$

Fermi momentum: $p_f = \sqrt{2m_n E_f} \approx 240 \text{ MeV}$

RMS neutron angle: $\sigma_\theta = \frac{p_f}{2p_{\text{beam}}/A} = 44 \text{ } \mu\text{rad}$ (ALICE ZDC Monte Carlo gives 51 μrad)

Compare collisional beam at IP: $\sigma_{p_y} = \sqrt{\frac{\epsilon_n}{2\beta^* \sqrt{2\gamma^2 - 1}}} \approx 22.5 \text{ } \mu\text{rad}$

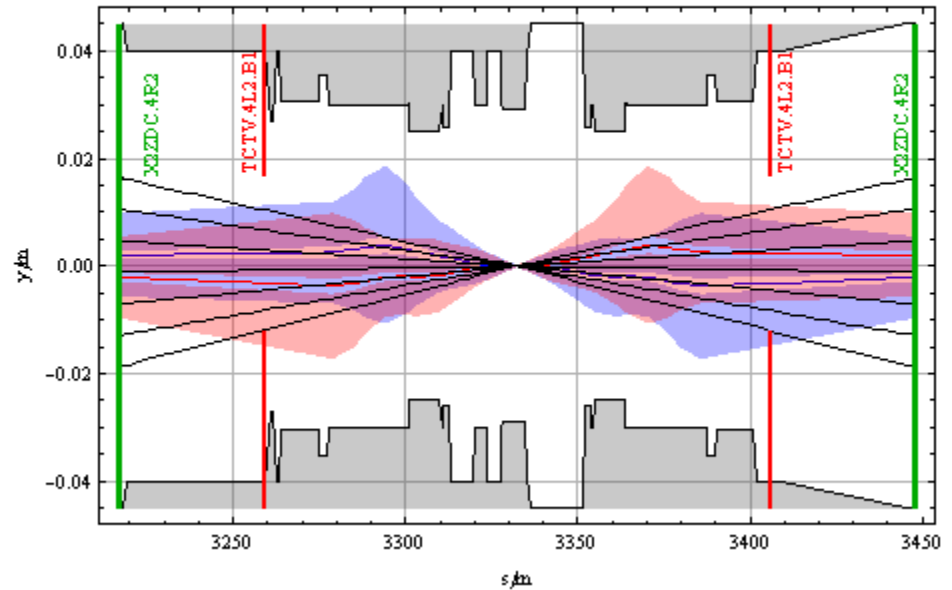
Neutrons are not focussed in straight sections (no strong sextupoles!).

In electromagnetic dissociation, mean transverse momentum is less, 27 MeV/c.

Nominal ion collision optics ($\beta^*=0.5$ m, 10 μ rad crossing angle)

- Black lines show $\pm 0, 1, 2, 3\sigma$ of neutron beam (3σ includes 98.9% of flux).
- Blue is vertical beam (8.3σ) envelope of Beam 1 (L \rightarrow R), pink is Beam 2 (R \rightarrow L).
- Closed orbit tolerance is hollowed out around closed orbit line in centre of beam envelope (about 1σ).
- TCTV collimators shown in red, jaws are centred on closed orbit, at 13σ in this case (previously 8.3).
- Planes of ZDC detectors shown in green.

($8.3\sigma_x, 8.3\sigma_y, 5\sigma_z$) envelope for $\epsilon_x = 5.02646 \times 10^{-10}$ m, $\epsilon_y = 5.02646 \times 10^{-10}$ m, $\sigma_z = 0.0001137$
 and closed orbit tolerance ($0.0000223607\sqrt{\beta_x m}, 0.0000223607\sqrt{\beta_y m}$)

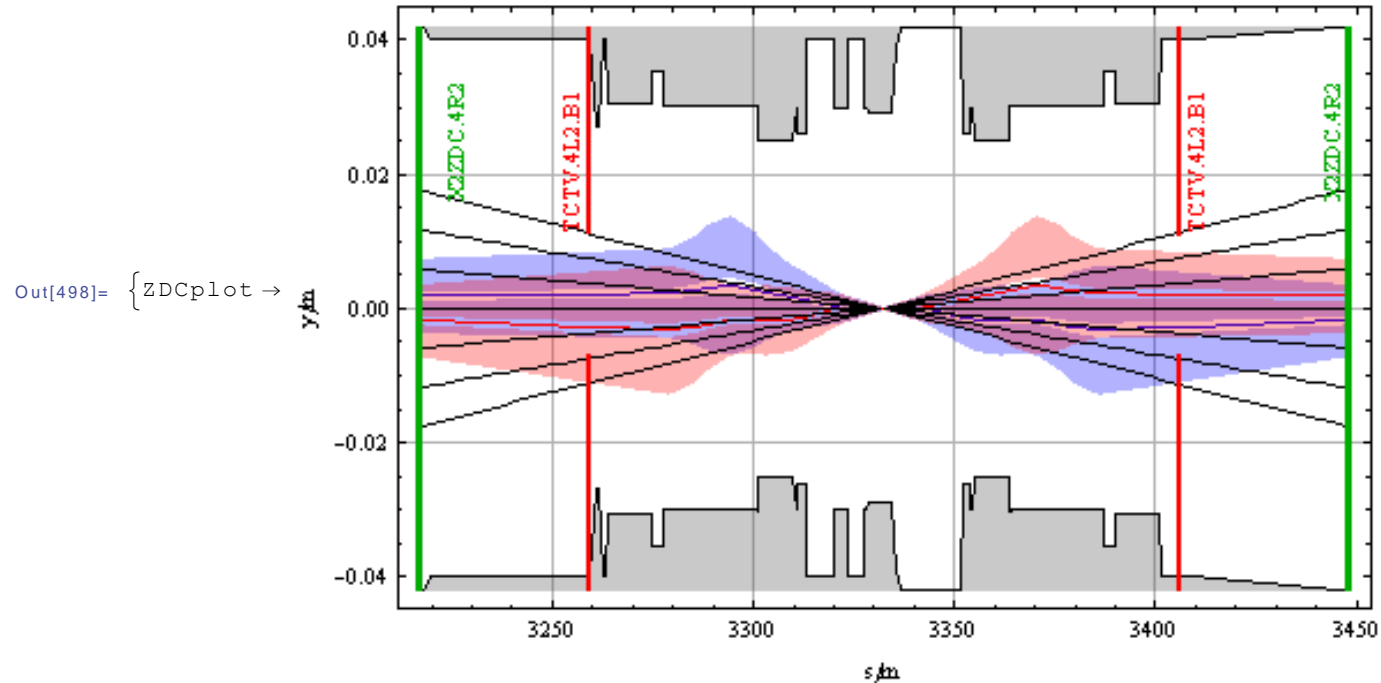


```
CrossingAngles → {2.62512 × 10-12, -0.00001, 5.49839 × 10-12, 0.00001},
nSigmaTCT → 15., jawTCT →
{{TCTV.4L2.B1, {0.016789, -0.0119541}}, {TCTV.4R2.B2, {0.0167375, -0.0119175}}}
```

Early ion collision optics ($\beta^* = 1. \text{ m}$, zero crossing angle)

($8.3\sigma_x, 8.3\sigma_y, 5.\sigma_z$) envelope for $\epsilon_x = 5.02646 \times 10^{-10} \text{ m}$, $\epsilon_y = 5.02646 \times 10^{-10} \text{ m}$, $\sigma_z = 0.0001137$

and closed orbit tolerance ($0.0000223607\sqrt{\beta_x \text{ m}}$, $0.0000223607\sqrt{\beta_y \text{ m}}$)



CrossingAngles → $\{-1.82661 \times 10^{-12}, -2.13464 \times 10^{-12}, 1.16206 \times 10^{-14}, -3.55563 \times 10^{-13}\}$,

nsigmaTCT → 13., jawTCT →

$\{\{\text{TCTV.4L2.B1}, \{0.0109789, -0.00672659\}\}, \{\text{TCTV.4R2.B2}, \{0.0109474, -0.00670726\}\}\}$

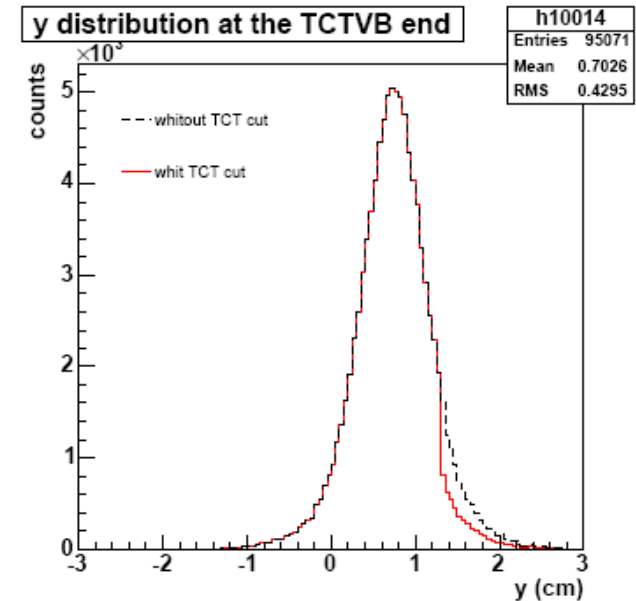
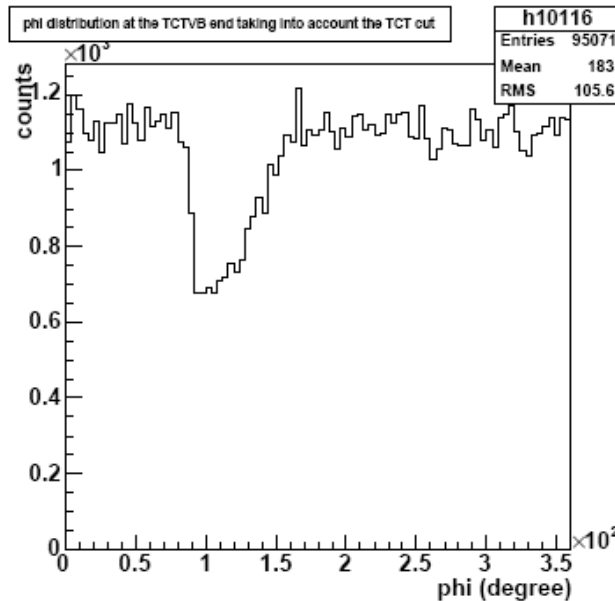
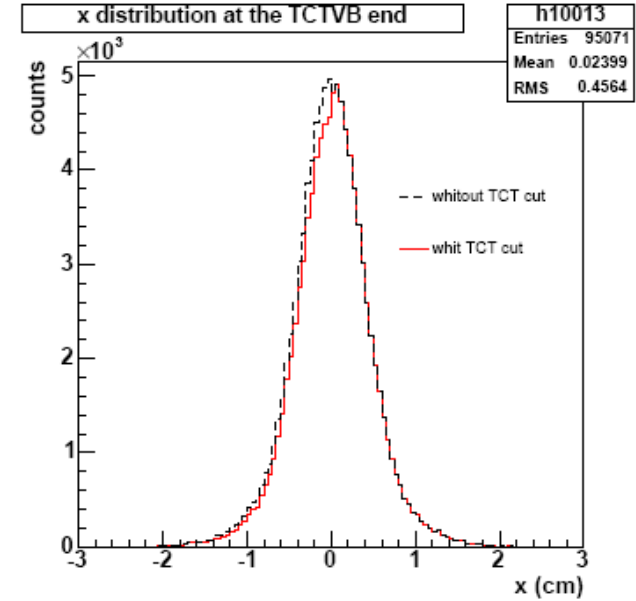
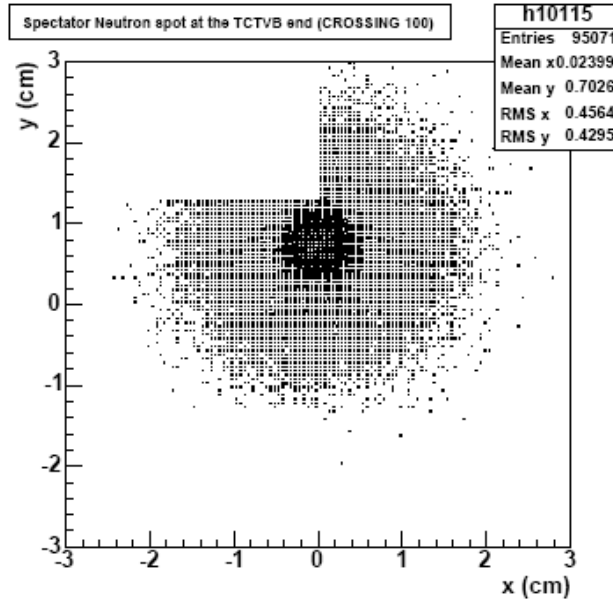
Because beam is smaller, a $\pm 13\sigma$ collimator gap is not enough to let the neutron beam pass.

As in the nominal optics, the neutrons are not centred on the collimator gap.

TCTVB neutron shadow on ZDC for 100 μ rad crossing angle

100 microrad crossing angle at IP2 with 30 microrad beam divergence (larger than we are likely to use in heavy-ion operation).

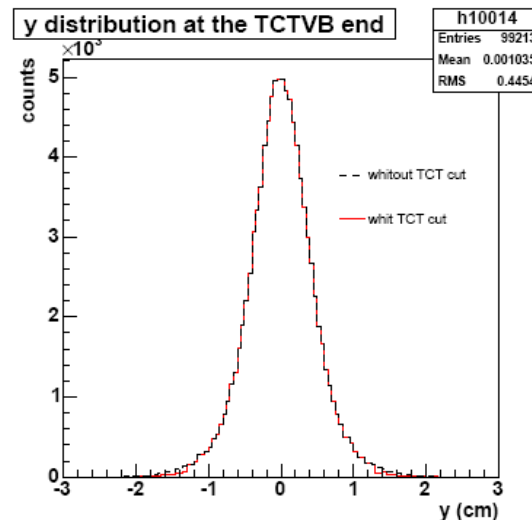
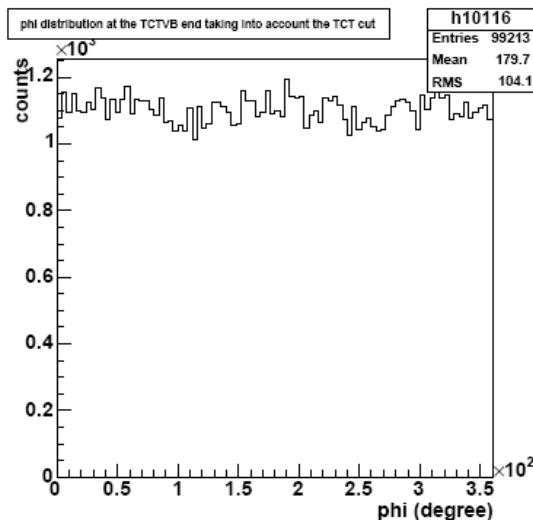
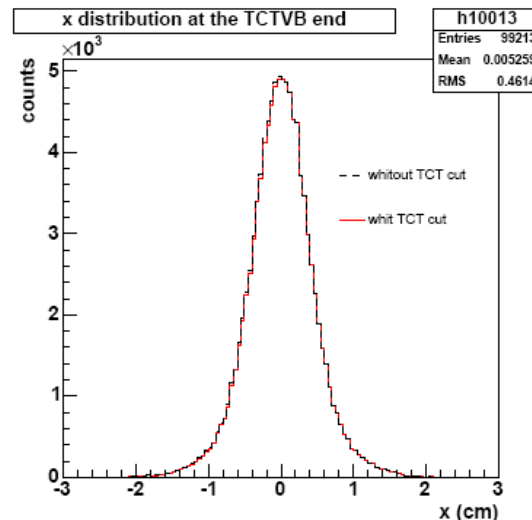
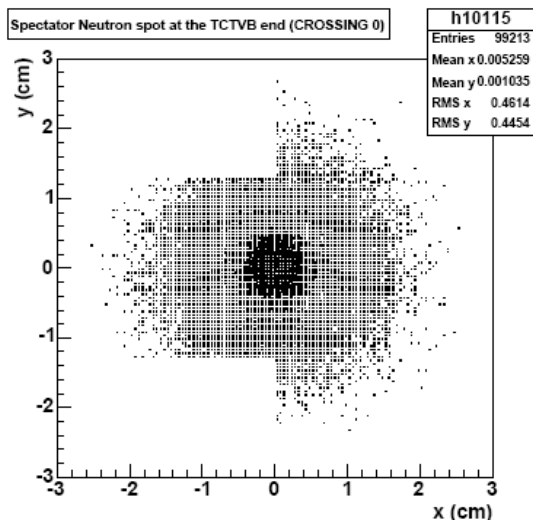
The number of spectator neutrons hitting the jaws is 5% and the ϕ distribution is not flat



From M. Gallio et al

TCTVB neutron shadow on ZDC for zero crossing angle

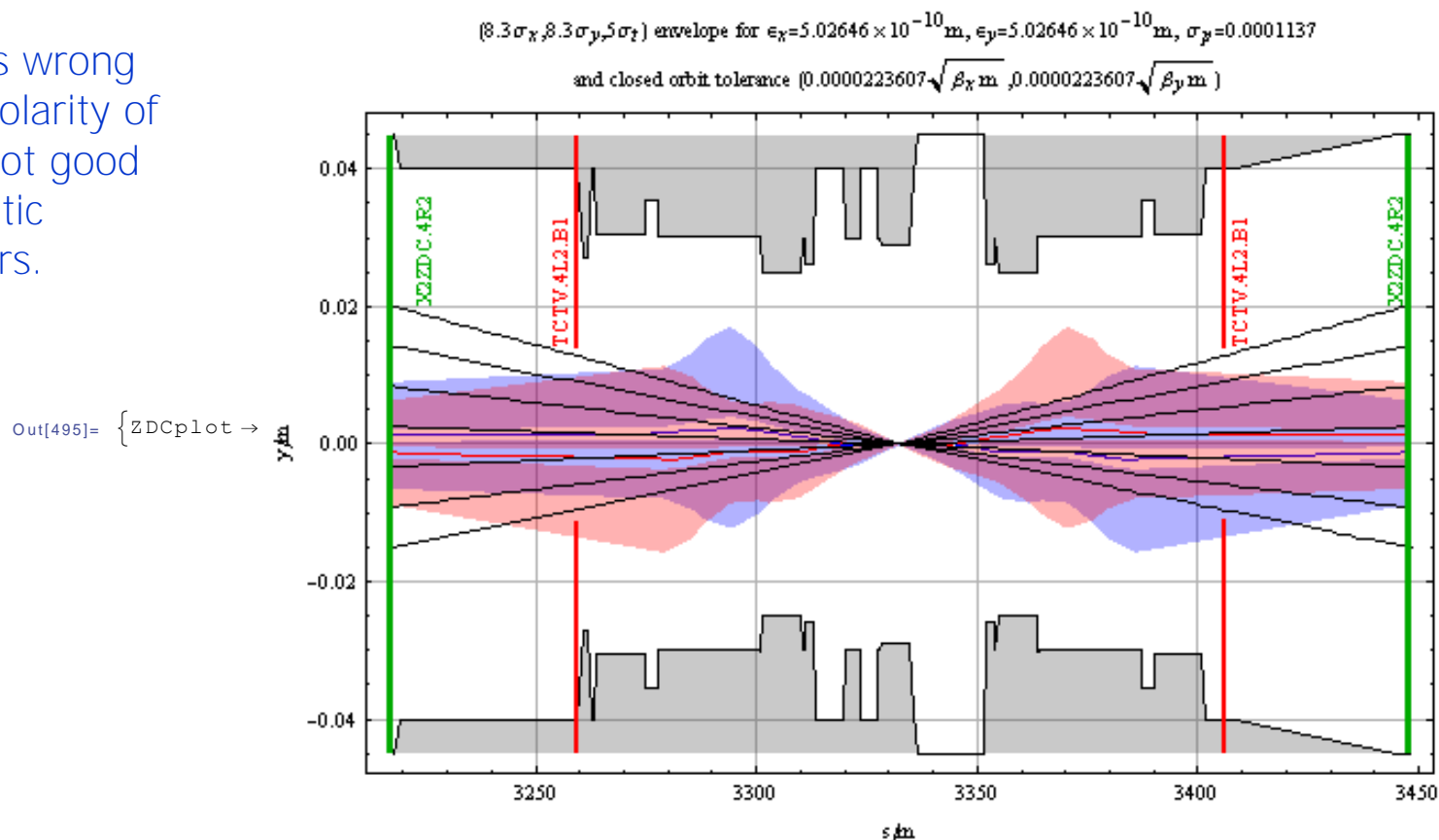
Zero crossing angle at IP2 with 30 microrad beam divergence. The number of spectator neutrons hitting the jaws is 0.8% and the ϕ distribution appears flat.



From M. Gallio et al

Optimum for Nominal Ion Collision Optics at $\sim 20 \mu\text{rad}$

But this is wrong
relative polarity of
bumsp, not good
for parasitic
encounters.



```

CrossingAngles -> {1.28934 x 10-12, 0.000022, 6.83363 x 10-12, -0.000022}, nsigmaTCT -> 13,
jawTCT -> {{TCTV.4L2.B1, {0.0139058, -0.0110049}}, {TCTV.4R2.B2, {0.0138632, -0.0109711}}},
MADfile -> CollisionIons60.madx, LHCB1opticsFile -> LHCB1CollisionIons60.tfs,
LHCB2opticsFile -> LHCB2CollisionIons60.tfs,
MADXterminalOutputFile -> CollisionIons60.mou, ON_X2 -> 0.6}
    
```

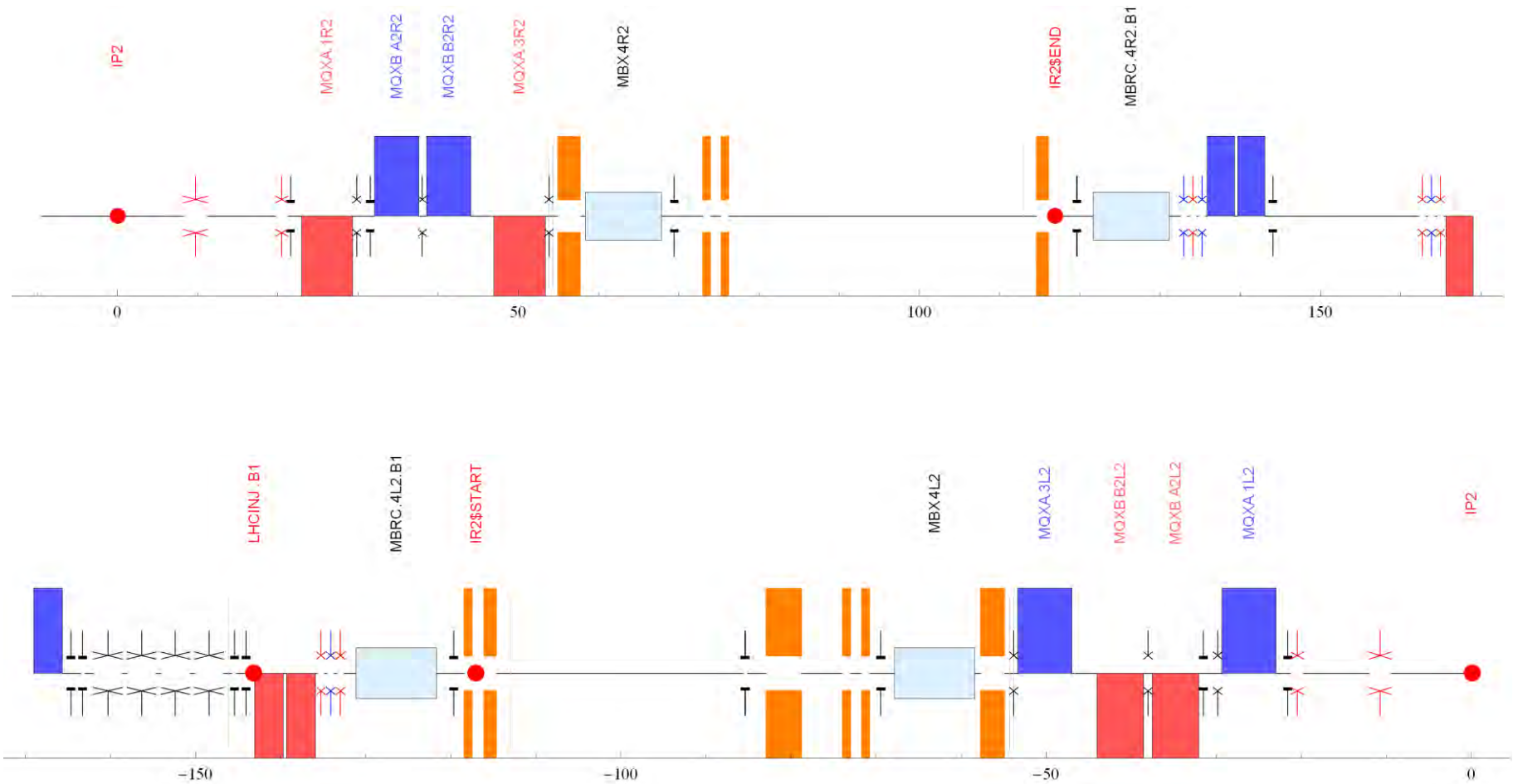
Previous conclusions (discussions with ALICE)

- With the assumptions on collimator gap settings, there are new optimum crossing angles, depending only weakly on β^* , that will allow a maximum neutron flux to pass
 - Re-consider running configuration for heavy-ions in ALICE
 - Can we use ZDC data in setting up collision conditions?
- Most straightforward solution is to simply withdraw TCTV collimators
 - No failure scenario for vertical orbit ?
- Alternative would be to rearrange hardware to put TCTVs behind ZDC
 - Analyse that now ...

Approach

- Geometry of the vacuum chambers in the separation region
 - Build 3D model from layout drawings rather than complicated patching of MAD aperture description
 - This is in global cartesian coordinates
- Geometry of the beam
 - Beam envelopes calculated in Courant-Snyder (CS) coordinate system
 - Use transformations from CS system to global cartesian frame to place the beam in 3D chamber model
- Consider implications of moving y-chamber towards IP to make room for TCTVB behind ZDC
 - Operations naturally carried out in global cartesian frame

Schematic layouts right and left IR2



(In Mathematica notebook interface, mouse-over displays name of every element.)

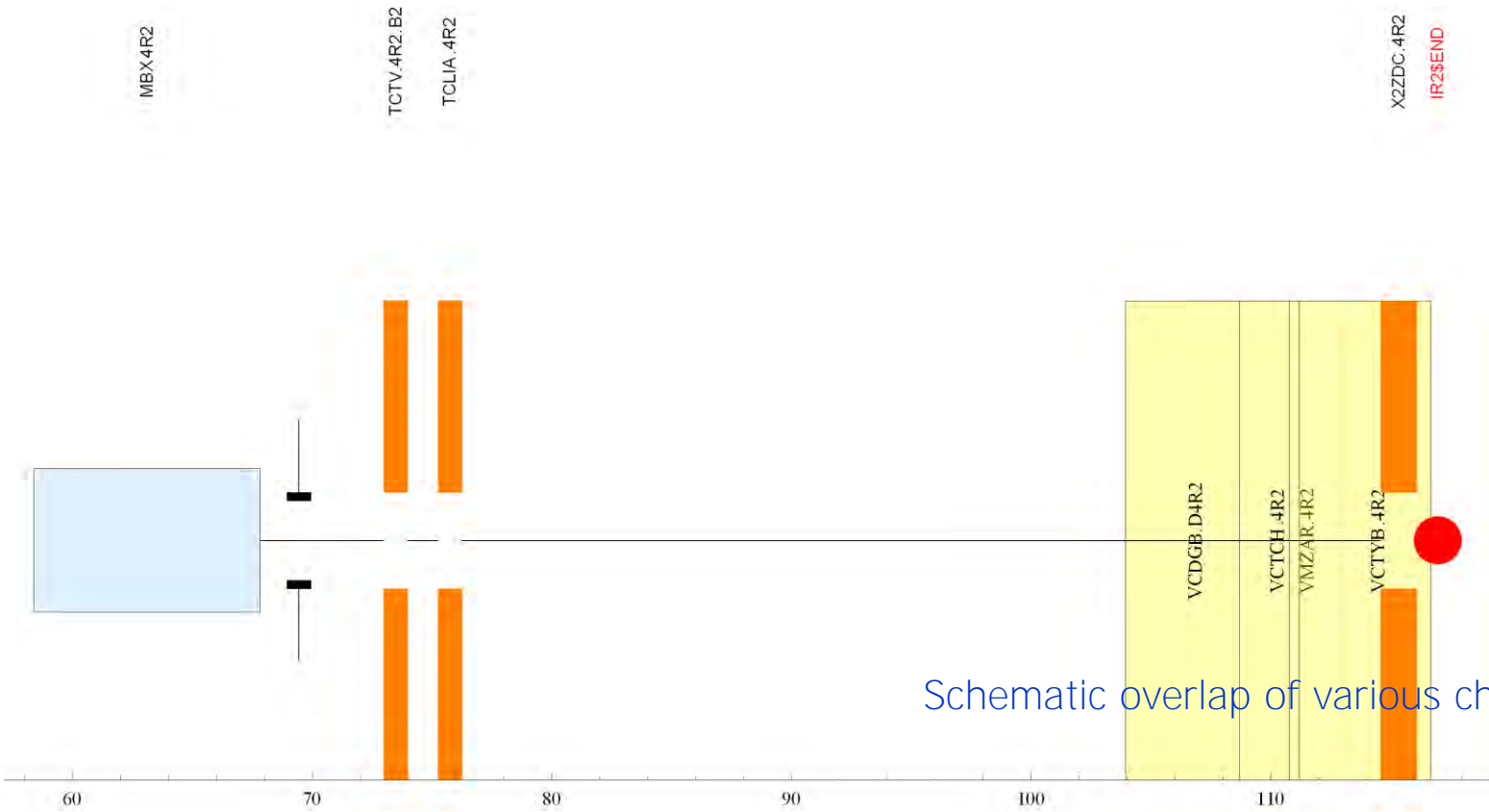
Vacuum chamber descriptions

Vacuum module name	distance from IP2 (m)	Comments
VCTYD.4L2	111.1930 - 116.6930	recombination chamber
VMZAR.4L2	110.7930 - 111.1930	bellow ID 196 mm
VCTCR.4L2	108.7030 - 110.7930	transition cone from ID 196 mm to ID 797 mm
VCDGA.D4L2	104.4310 - 108.7030	part of the ~ 20 m long chamber 797 mm ID
VCDGB.D4R2	103.9510 - 108.7030	part of the ~ 20 m long chamber 797 mm ID
VCTCH.4R2	108.7030 - 110.7930	transition cone from ID 196 mm to ID 797 mm
VMZAR.4R2	110.7930 - 111.1930	bellow ID 196 mm
VCTYB.4R2	111.1930 - 116.6930	recombination chamber

From D. Macina

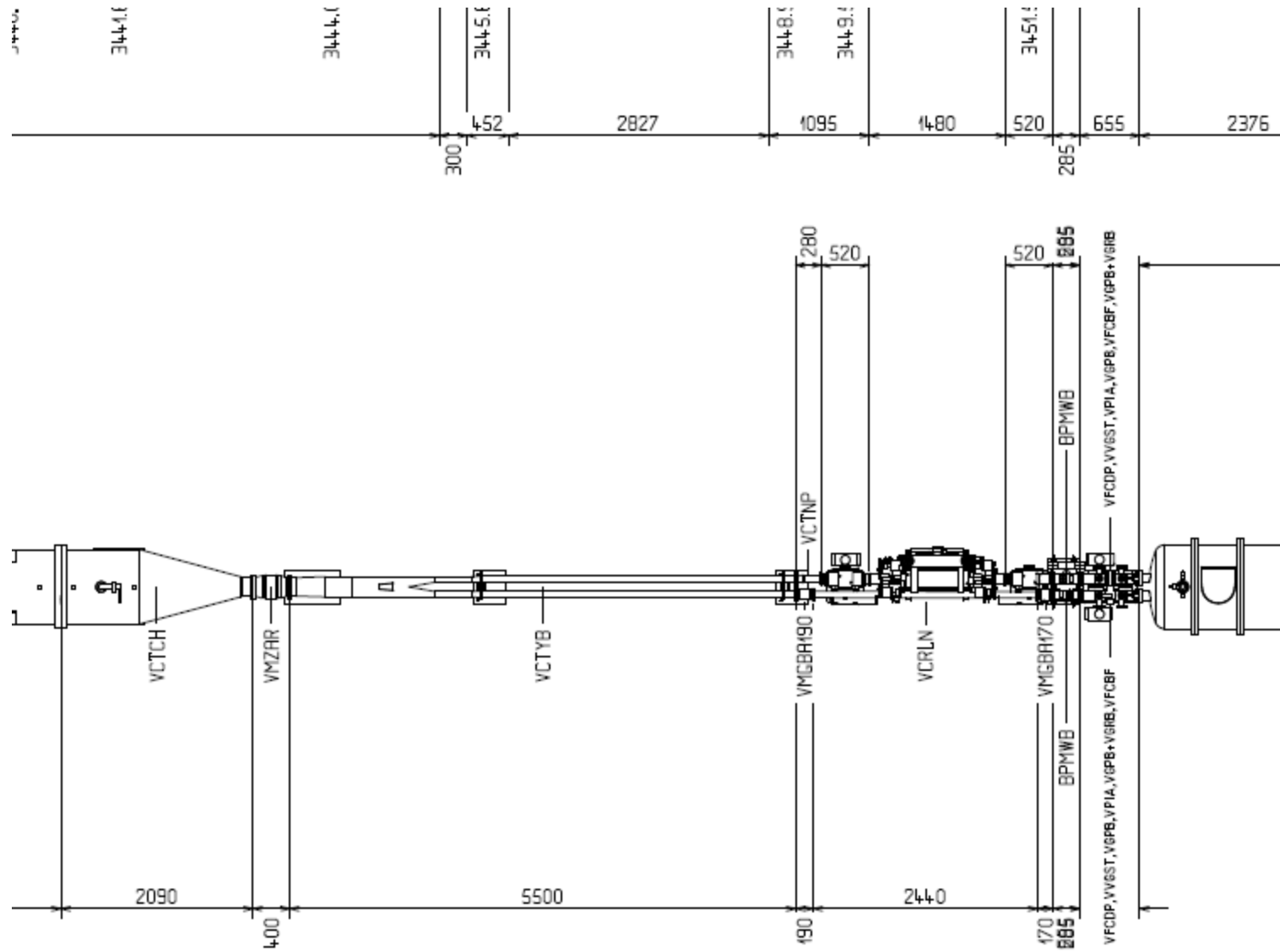
The big vacuum chamber (ID 797 mm) in LSS2L is tilted on the horizontal plane to match the TDI which is displaced with respect to the beam axis for ALICE ZDC aperture reasons. You will notice in fact that there is an offset in the horizontal plane (U column, units are meters, + is towards machine center) and an angle with respect to the beam axis (C column).

Close-up of y-chamber region

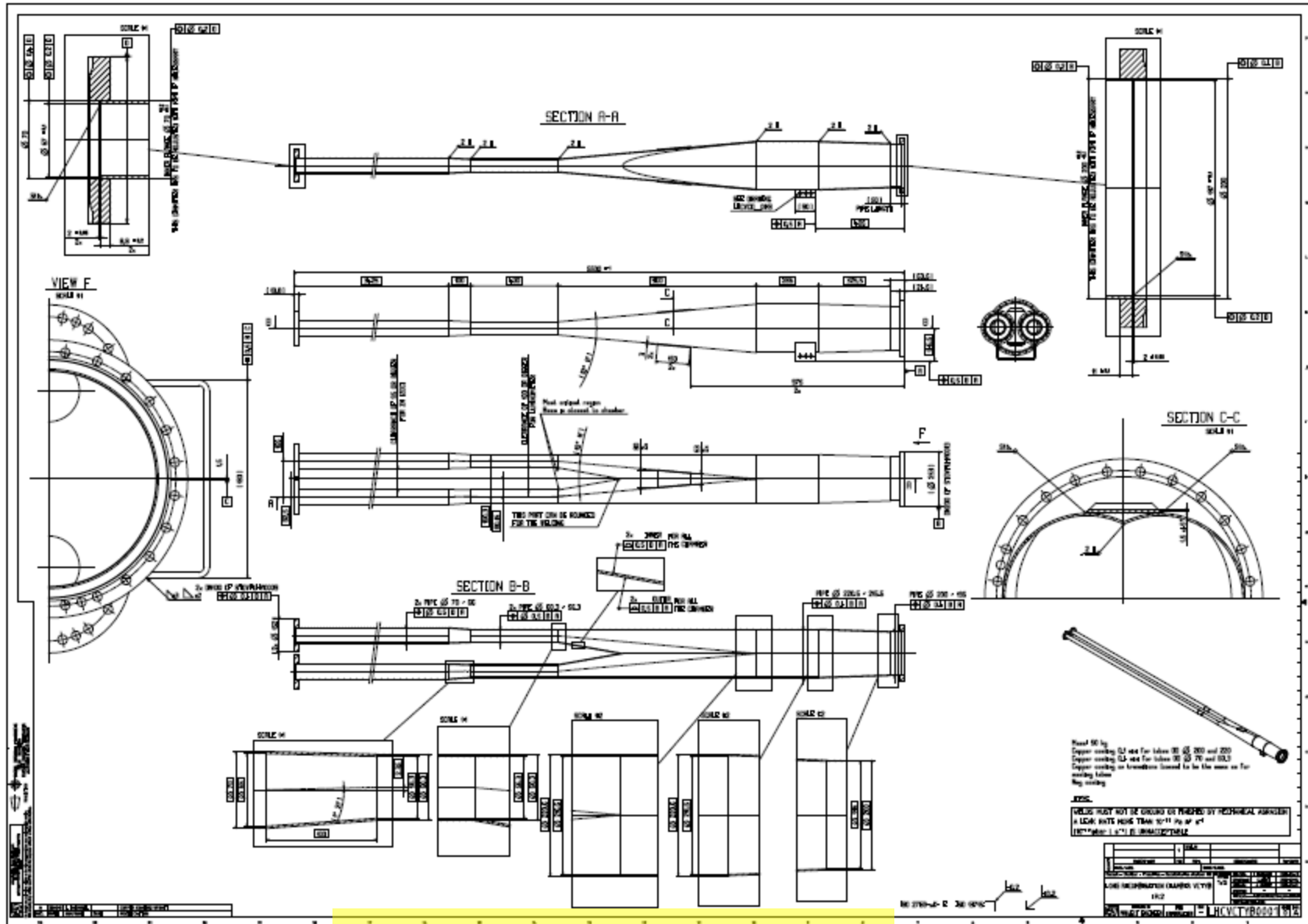


Schematic overlap of various chambers

Drawing of the region

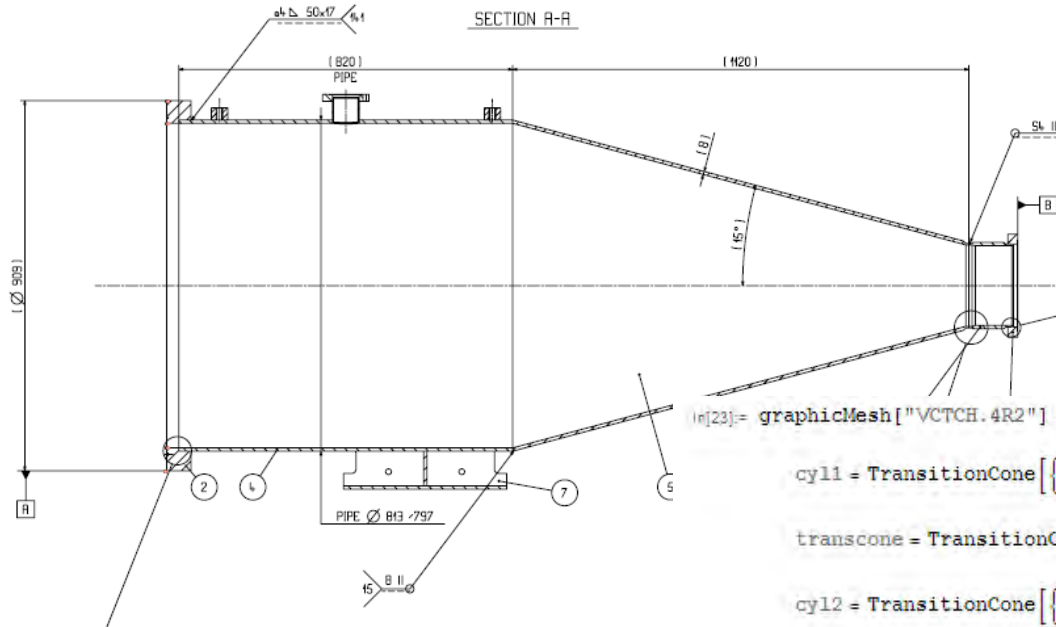


Drawing of y-chamber



Translated into description as Graphics3D objects in Mathematica

Transition cone example

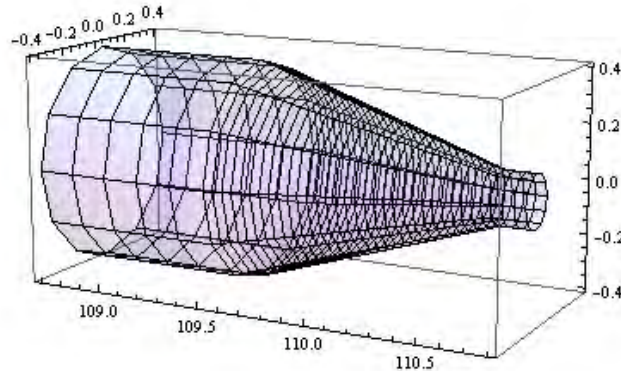


```

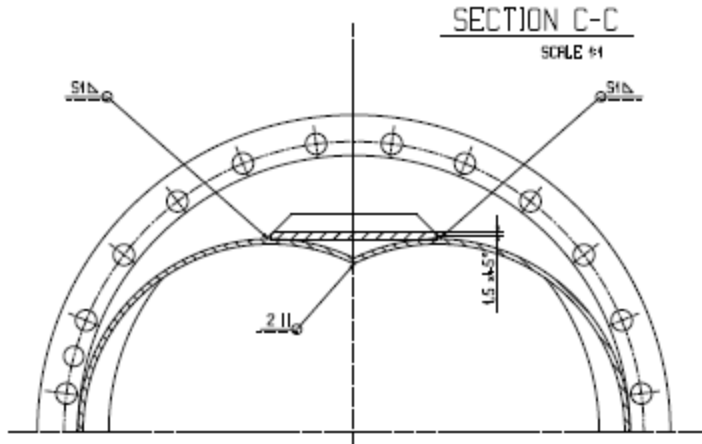
In[23]= graphicMesh["VCTCH.4R2"] = Module[{cy11, transcone, cy12},
  cy11 = TransitionCone[{108.703^-, 797. 10^-3}, {108.703^+ + 0.820, 797. 10^-3}, 5];
  transcone = TransitionCone[{108.703^+ + 0.820, 797. 10^-3}, {108.703^+ + 0.820 + 1.120, 196. 10^-3}, 30];
  cy12 = TransitionCone[{108.703^+ + 0.820 + 1.120, 196. 10^-3}, {110.793^-, 196. 10^-3}, 3];
  Join[cy11, transcone, cy12];

ListPlot3D[graphicMesh["VCTCH.4R2"], PlotStyle -> Opacity[0.2]]

```



y-chamber



Various transition cones combined with
 Parametric description of transition from
 single large cylindrical pipe to two separate
 pipes

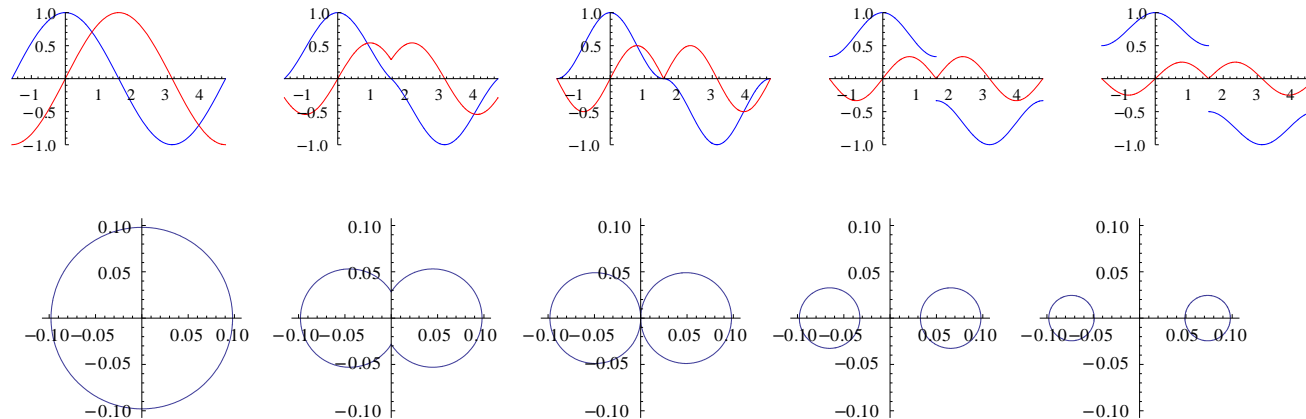
`ychamberx[r1, r, θ] // TraditionalForm`

$$\begin{cases} \cos\left(\frac{\theta(2 \sin^{-1}(\min(1, \frac{r1-r}{r})) + \pi)}{\pi}\right) r - r + r1 & -\frac{\pi}{2} \leq \theta \leq \frac{\pi}{2} \\ \cos\left(\frac{2 \sin^{-1}(\min(1, \frac{r1-r}{r}))\theta + \pi\theta - 2\pi \sin^{-1}(\min(1, \frac{r1-r}{r}))}{\pi}\right) r + r - r1 & \frac{\pi}{2} \leq \theta \leq \frac{3\pi}{2} \end{cases}$$

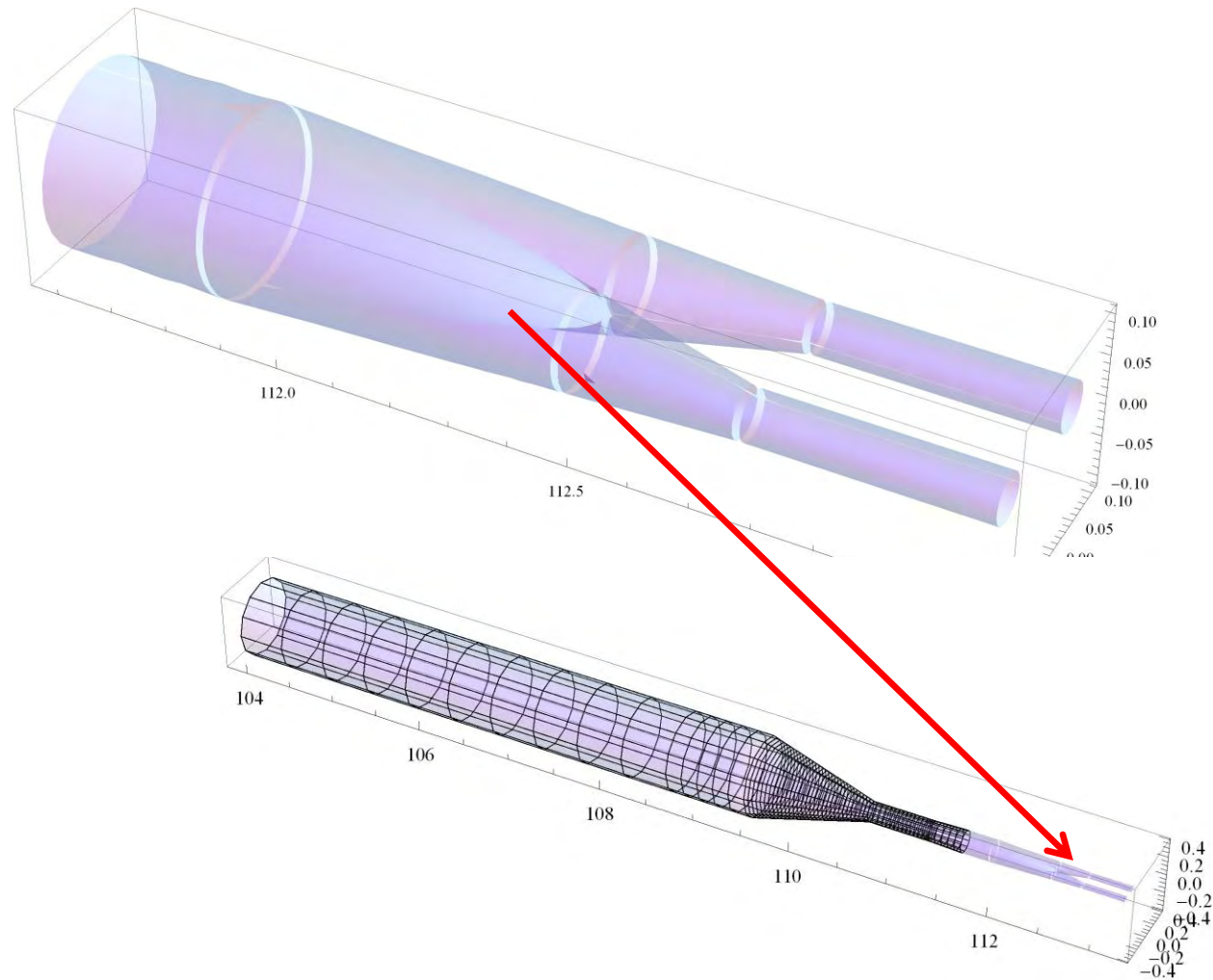
`ychambery[r1, r, θ] // TraditionalForm`

$$\begin{cases} r \sin\left(\frac{\theta(2 \sin^{-1}(\min(1, \frac{r1-r}{r})) + \pi)}{\pi}\right) & -\frac{\pi}{2} \leq \theta \leq \frac{\pi}{2} \\ r \sin\left(\frac{2 \sin^{-1}(\min(1, \frac{r1-r}{r}))\theta + \pi\theta - 2\pi \sin^{-1}(\min(1, \frac{r1-r}{r}))}{\pi}\right) & \frac{\pi}{2} \leq \theta \leq \frac{3\pi}{2} \end{cases}$$

Out[138]//Short=

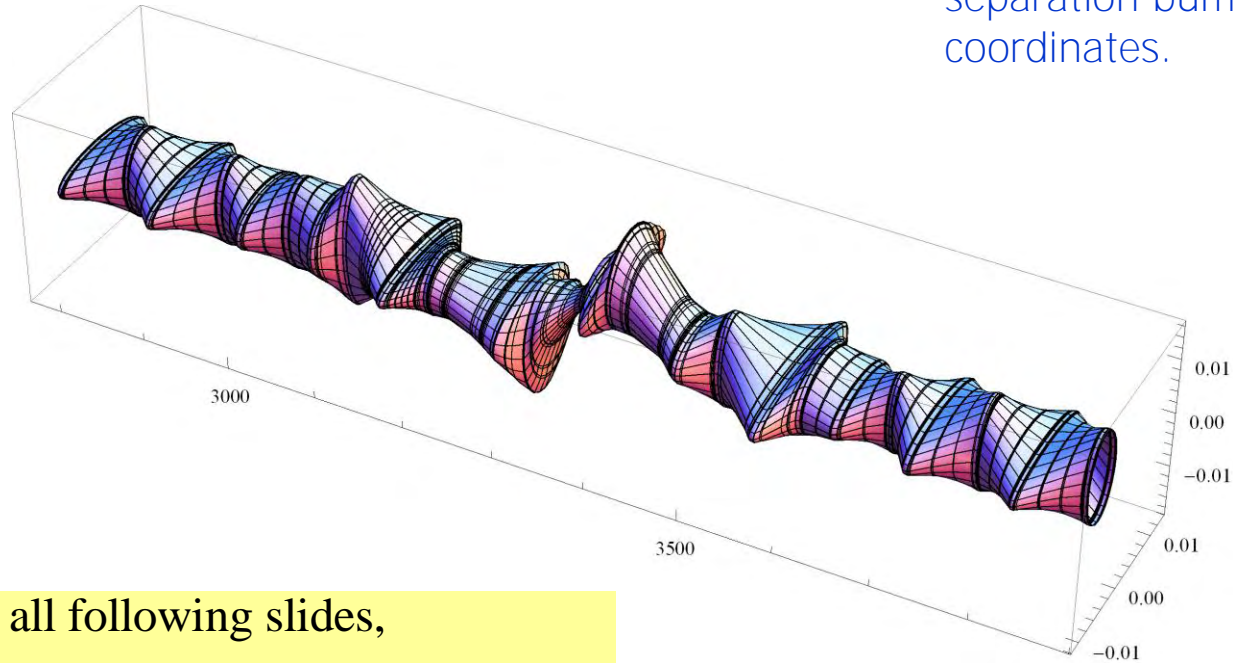


Y-chamber and combined chambers in 3D



Injection circulating beam envelope in CS coordinates

The axis of this envelope appears straight (except for the separation bumps) in the CS coordinates.



Here and in all following slides,
we show the $(7\sigma_x, 7\sigma_y, 5\sigma_t)$ beam envelope.

Mathematica function for CS to global transformations

CStoGlobal returns a function which, when acting on a point $\{x,y,z\}$ in the local Courant–Snyder coordinate system, transforms it to the global cartesian system according according to the Euclidean group parameters X,Y,Z,θ,ϕ,ψ obtained from the various forms of its arguments.

CStoGlobal $[X,Y,Z,\theta,\phi,\psi]$ specifies them directly;

CStoGlobal[surv,element] gets the Euclidean group parameters at a given element contained in the mfs SURVEY data object surv;

CStoGlobal[fsurv,s] takes a list of 6 InterpolatingFunction or Function objects and evaluates them at s to get the Euclidean group parameters where, typically, fsurv is constructed from mfs SURVEY data using mfsSurveyInterpolation.

The inverse function GlobaltoCS works similarly. >>

Several forms of argument (“overloading”).

Connects MAD SURVEY type data to beam-dynamics coordinates, beam envelopes, etc.

Any s value works (not just ends of elements).

(Some people would call CStoGlobal a *functional* since it returns a function.)

Examples

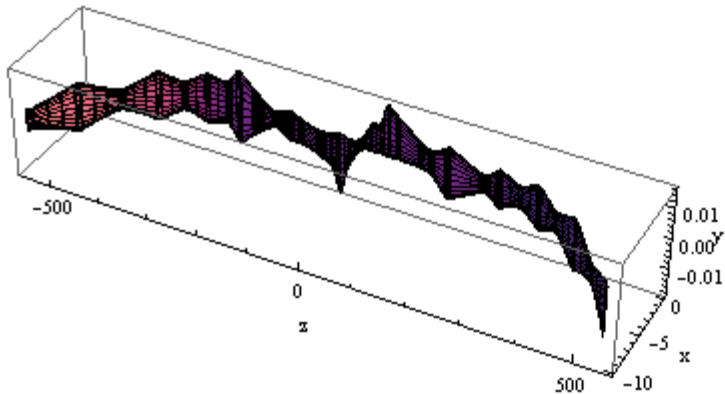
```
CStoGlobal[X, Y, Z,  $\frac{\pi}{5}$ ,  $\frac{\pi}{3}$ ,  $\psi$ ]@{x, y, z} // Simplify // MatrixForm
```

$$\begin{pmatrix} \frac{1}{8} \left(8X + \sqrt{10 - 2\sqrt{5}} z + \left(2(1 + \sqrt{5})x - \sqrt{30 - 6\sqrt{5}} y \right) \cos[\psi] - \left(\sqrt{30 - 6\sqrt{5}} x + 2(1 + \sqrt{5})y \right) \sin[\psi] \right) \\ \frac{1}{2} \left(2Y + \sqrt{3} z + y \cos[\psi] + x \sin[\psi] \right) \\ \frac{1}{8} \left(z + \sqrt{5} z + 8Z - \left(2\sqrt{10 - 2\sqrt{5}} x + \sqrt{3} (1 + \sqrt{5}) y \right) \cos[\psi] - \left((\sqrt{3} + \sqrt{15}) x - 2\sqrt{10 - 2\sqrt{5}} y \right) \sin[\psi] \right) \end{pmatrix}$$

```
CStoGlobal[LHCB1IR2Survey, "IP2"]@{x, y, z} // MatrixForm
```

$$\begin{pmatrix} -1231.44 + 0.707107 x - 0.707107 z \\ y \\ 2973.29 + 0.707107 x + 0.707107 z \end{pmatrix}$$

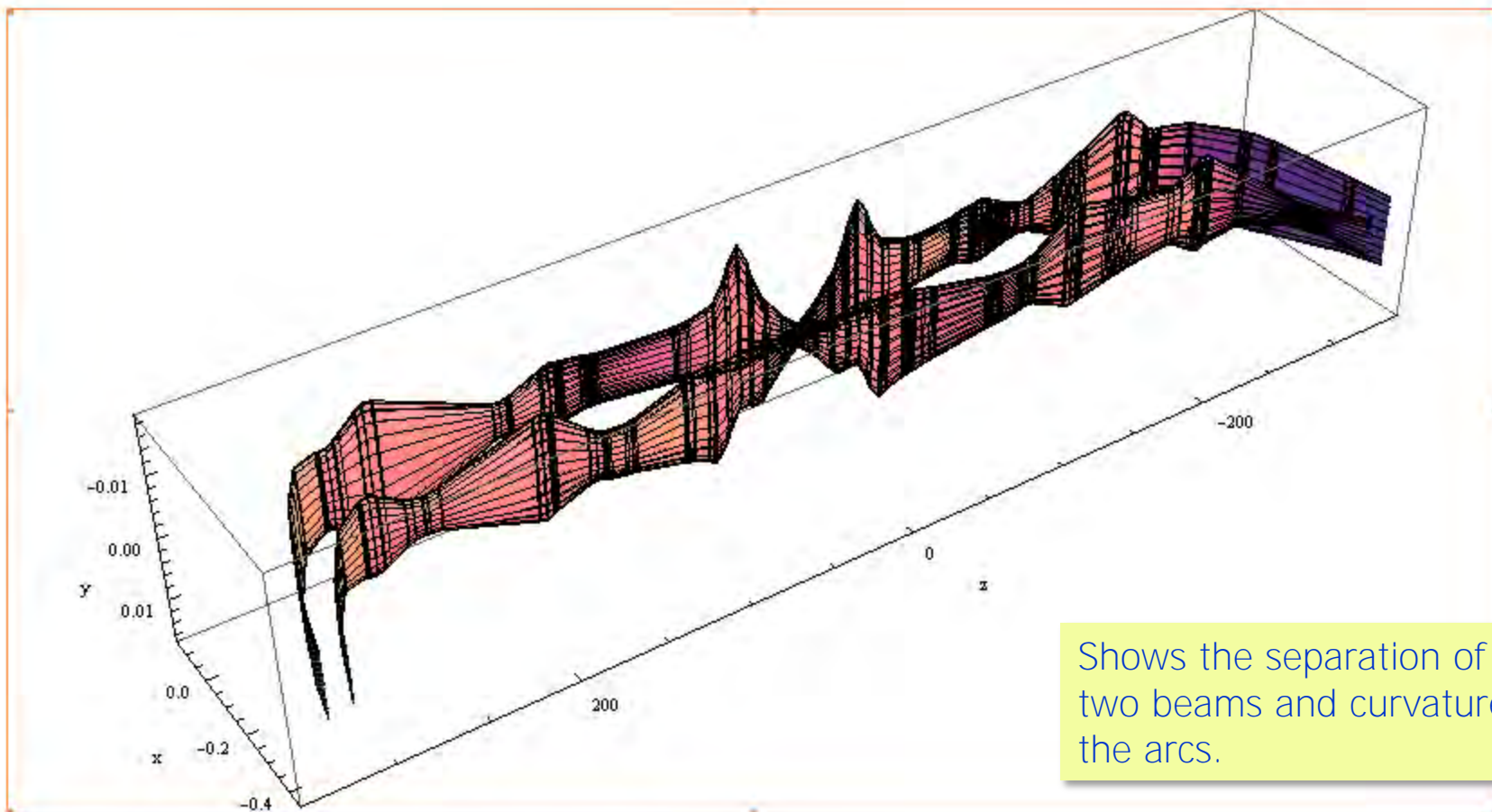
```
LHCB2InjectionOpticsEnvelopeGlobal =
  LHCB2InjectionOpticsEnvelopeLocal /.
    {s_, x_, y_} => GlobaltoCS[LHCB2IR2Survey, "IP2"]@
      CStoGlobal[fLHCB2IR2Survey, s]@{x, y, 0} /. {X_, Y_, Z_} -> {Z, X, Y};
ListPlot3D[LHCB1InjectionOpticsEnvelopeGlobal, BoxRatios -> {5, 1, 1},
  AxesLabel -> {"z", "x", "y"}]
```



This example transforms all points in a beam envelope surface computed in CS coordinates. The inverse transformation at IP2 relocates the origin of the global frame from IP1 to IP2, letting us see the curvature of Beam 1 orbit around IR2 on a suitable scale.

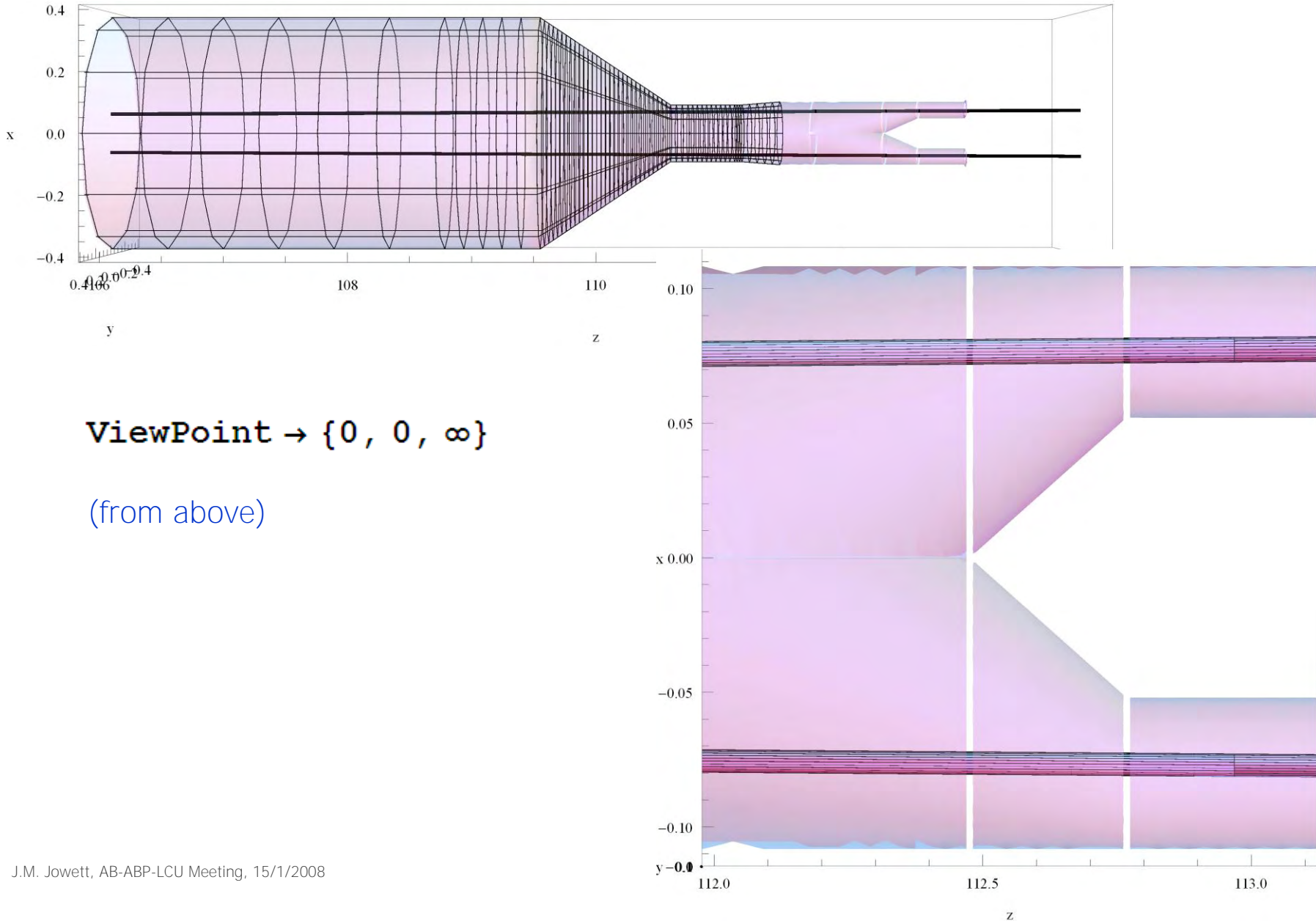
Combining beam envelopes in a cartesian frame

```
Show[
  {ListPlot3D[LHCB1InjectionOpticsEnvelopeGlobal, BoxRatios -> {5, 1, 1}, AxesLabel -> {"z", "x", "y"},
    PlotRange -> {350 {-1, 1}, 0.15 {-3, 1}, All}},
  ListPlot3D[LHCB2InjectionOpticsEnvelopeGlobal]
}, ViewPoint -> Front
]
```



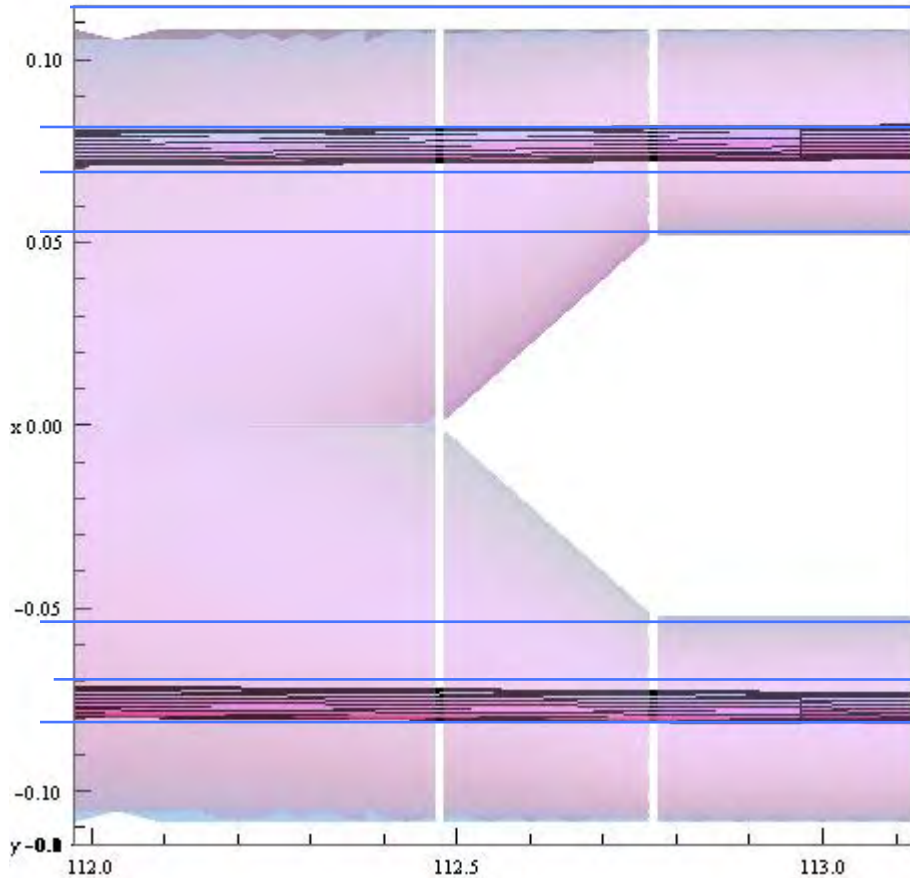
Shows the separation of the two beams and curvature of the arcs.

Beam envelopes in the y-chamber region R2

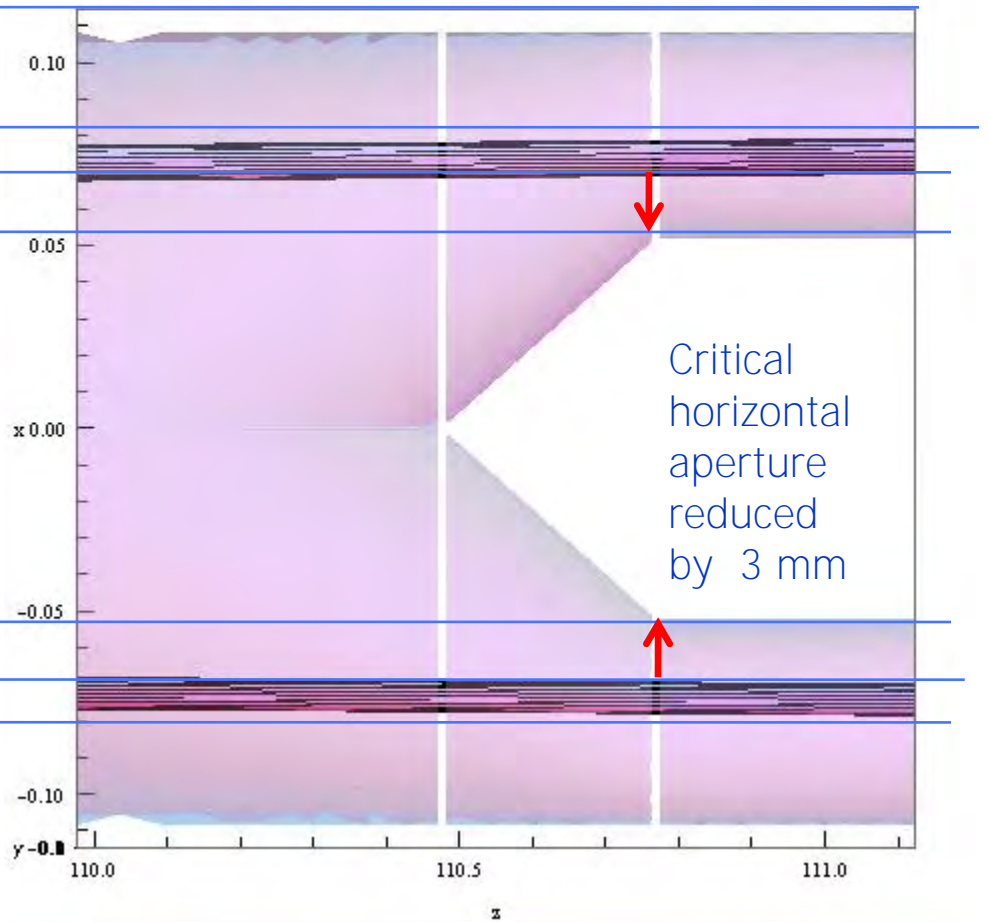


Move chamber (R2) by 2 m towards IP2

```
Show[
  {ListPlot3D[LHCB1InjectionOpticsEnvelopeGlobalShort],
   ListPlot3D[LHCB2InjectionOpticsEnvelopeGlobalShort],
   Graphics3D[graphic3D["chamberR2"]]}
, ViewPoint -> {0, 0, Infinity}, BoxRatios -> {1, 1, 1}, AxesLabel -> zxy,
PlotRange -> {{112., 113.1}, {-0.11, 0.11}, 0.15 {-1, 1}}
]
```



```
Show[
  {ListPlot3D[LHCB1InjectionOpticsEnvelopeGlobalShort],
   ListPlot3D[LHCB2InjectionOpticsEnvelopeGlobalShort],
   Graphics3D[Translate[graphic3D["chamberR2"], {-2, 0, 0}]}]}
, ViewPoint -> {0, 0, Infinity}, BoxRatios -> {1, 1, 1}, AxesLabel -> zxy,
PlotRange -> {{112., 113.1} - 2, {-0.11, 0.11}, 0.15 {-1, 1}}
]
```



Same thing “analytically”

The local transformation in the critical region allows us to calculate the position of the closed orbit.

```
: GlobaltoCS[LHCB1IR2Survey, "IP2"]@CStoGlobal[fLHCB1IR2Survey, sIP2 + 112.76]@{x, y, z} //  
Simplify // Chop // MatrixForm
```

```
MatrixForm=  

$$\begin{pmatrix} -0.0760921 + 0.999999 x - 0.0015325 z \\ 1. y \\ 112.76 + 0.0015325 x + 0.999999 z \end{pmatrix}$$

```

At the corresponding position with respect to the shifted chamber:

```
= GlobaltoCS[LHCB1IR2Survey, "IP2"]@  
CStoGlobal[fLHCB1IR2Survey, sIP2 + 112.76 - 2]@{x, y, z} // Simplify // Chop //  
MatrixForm
```

```
MatrixForm=  

$$\begin{pmatrix} -0.0730271 + 0.999999 x - 0.0015325 z \\ 1. y \\ 110.76 + 0.0015325 x + 0.999999 z \end{pmatrix}$$

```

The 0.003 m difference in the constant term of the first component is the shift of the closed orbit towards the Z-axis of the cartesian frame with origin at IP2.

This can also be seen from the coefficient of z.

Summary

- We now have a geometric description of the beams and vacuum chambers in the y-chamber region
 - Tools can be applied to any other part of machine/transfer lines, etc, generally to relate beam coordinates to any global cartesian frame.
 - Could also be used to generate aperture description in MAD style
- Moving y-chamber 2 m towards IP to put TCTV behind ZDC reduces critical horizontal beam aperture in the y-chamber by 3 mm.
 - This is probably not acceptable but further checks are to be made.